Available online at www.sciencedirect.com
ScienceDirect
Journal of Power Sources 180 (2008) 143–153
JOURNAL OF POWER SOURCES
www.elsevier.com/locate/jpowsour

Proton conducting CS/P(AA-AMPS) membrane with reduced methanol permeability for DMFCs

Zhongyi Jiang, Xiaohong Zheng, Hong Wu *, Jingtao Wang, Yabo Wang

Key Laboratory for Green Chemical Technology, School of Chemical Engineering and Technology, Tianjin University, Tianjin 300072, China

Received 20 December 2007; received in revised form 18 January 2008; accepted 22 January 2008
Available online 6 February 2008

Abstract

A novel polyelectrolyte complex (PEC) membrane for direct methanol fuel cells (DMFCs) was prepared by blending a cationic polyelectrolyte, chitosan (CS), with an anionic polyelectrolyte, acrylic acid-2-acrylamido-2-methylpropane sulfonic acid copolymer (P(AA-AMPS)). The presence of $-NH_3^+$ species detected by X-ray photoelectron spectroscopy (XPS) revealed that an ionic cross-linked interpenetrating polymer network (IPN) was formed between the two polyelectrolyte polymers. Methanol permeability and proton conductivity were measured and compared with the Nafion®117 membrane. The dual function of P(AA-AMPS) as both an ionic crosslinker and a proton conductor led to not only a notable reduction in methanol permeability but also an increase in proton conductivity. The CS/P(AA-AMPS) membrane with a P(AA-AMPS) content of 41 wt.% exhibited a methanol permeability (P) of 2.41×10^{-7} cm^2 s^{-1} which was fifteen times lower than that of the Nafion®117 membrane, whereas its proton conductivity (σ) was comparatively high (3.59×10^{-2} S cm^{-1}). In terms of the overall selectivity index ($\beta = \sigma/P$), the PEC membrane showed a remarkably higher selectivity than the Nafion®117 membrane, and, furthermore, the overall selectivity index increased with the increase of P(AA-AMPS) content. The mechanism of proton transfer was tentatively discussed based on the activation energy of conductivity.

Keywords: Chitosan; P(AA-AMPS); DMFC membrane; Proton conductivity; Methanol permeability

1. Introduction

Direct Methanol Fuel Cells (DMFCs) are attracting much interest as an energy source for transport and other portable applications owning to its high energy density, simplified system design, convenient storage, recharge and transport of fuels [1]. Nafion®, a polyperfluorosulfonic acid ionomer developed by DuPont, has been intensively used in proton-exchange membrane fuel cells (PEMFCs), especially in the H_2/O_2 (air) fuel cells with success. Nafion® membranes exhibit excellent properties in terms of proton conductivity and chemical stability. However, two "high" drawbacks, high methanol crossover and high cost, limit its wide applications in DMFCs [2,3].

Polyelectrolyte complex (PEC) membranes with lower methanol crossover and manufacture cost have been demonstrated as promising candidates for DMFCs application. Presently, most of the current PEC membranes are based on hydrocarbon polymers typically encompassing sulfonated poly(ether ether ketone) (sPEEK), sulfonated poly(arylene ether sulfone) (sPAES), chitosan and poly(amide imide) (PAI) [4–7]. The interpenetrating polymer network (IPN) usually constructed within PEC membranes leads to an enhanced compatibility between the two polymers and thus a synergistic effect to suppress methanol crossover [8–11]. Some strong acids including sulfuric acid, phosphoric acid and heteropolyacid are often doped into the PEC matrix to increase the proton conductivity [12,13]. However, the accompanying decreased conductivity and the acid leaching-induced corrosion constitute the two inherent drawbacks. Membranes with an IPN structure formed by a cationic polyelectrolyte and an anionic polyelectrolyte may offer a feasible solution to obtain both low methanol crossover and high proton conductivity.

Chitosan, a cationic polyelectrolyte, is of growing interest in DMFCs membrane development [14,15]. The hydrophilic nature of chitosan ensures a high selectivity for water in the pervaporative separation of alcohol–water mixtures [16]. Herein,

* Corresponding author. Tel.: +86 22 27892143; fax: +86 22 27892143.
E-mail address: wuhong2000@gmail.com (H. Wu).

0378-7753/$ – see front matter © 2008 Elsevier B.V. All rights reserved.
doi:10.1016/j.jpowsour.2008.01.049

chitosan was chosen as the cationic polyelectrolyte for the fabrication of PEC membranes for its dual function as an alcohol barrier and a proton conductor, and the functional amino and hydroxyl groups on the polymer chains which were supposed to be utilized in constructing an IPN structure. In addition, chitosan, a deacetylation product of chitin obtained from crab and shrimp shells [14], is considered to be an extremely cheap, nonhazardous, and environmentally benign polymer. This will coincidently meet the requirements for replacing traditional hazardous power sources by the "green" fuel cells.

In addition, in the present study, a commercially available copolymer, (P(AA-AMPS)) composed of acrylic acid (AA) and AMPS with a high density of carboxyl and sulfonic groups, was chosen as the anionic polyelectrolyte in hopes of remarkably increasing the proton conductivity of the target membranes. As we know, the majority of anionic polyelectrolytes contains carboxyl (–COOH) or sulfonic ($–SO_3H$) groups [10,11,17,18]. For example, Poly(acrylic acid) (PAAc), a typical anionic polyelectrolyte, is known to entail a high charge density generated by a large amount of dissociated carboxyl groups. Polyelectrolyte complex of PAAc and chitosan has been prepared and assessed for applicability in DMFCs, and a low methanol permeability and a comparatively high proton conductivity were achieved [19]. Poly(2-acrylamido-2-methylpropane sulfonic acid) (PAMPS), another typical anionic polyelectrolyte with sulfonic groups ($–SO_3H$), has been prepared and employed in electrochromic devices as a proton conductor [20,21]. The conductivity of PAMPS was found to be higher than that of Nafion® under the same water content of $15H_2O$ per sulfonic acid group [22]. It has also been found that the ionic conductivity of PAMPS increases with water content up to $6H_2O$ per equivalent and then levels off [22]. This higher tolerance of the PAMPS polymer than Nafion® to the fluctuations in water content and drying ensures a higher ionic conductivity at a higher temperature or a lower water content. Okada and co-workers [23–25] have prepared complex membranes using PAMPS and poly(vinyl alcohol) (PVA) which displayed a comparable proton conductivity with Nafion®117. A number of new polymers based on the copolymerization of the AMPS monomer with other monomers have also been synthesized in recent years. The PAMPS-MMA polymer synthesized by free radical polymerization of methyl methacrylate (MMA) and AMPS has been tested as a DMFC membrane which displayed a comparable conductivity to Nafion® while the methanol permeability was much lower [26]. Another AMPS-based copolymer, AMPS-HEMA synthesized with AMPS and 2-hydroxyethyl methacrylate (HEMA), exhibited a high proton conductivity which was quite close to that of Nafion® [27]. The AMPS-HEMA copolymer was then blended with PVA to fabricate a proton conducting IPN. The resultant membrane exhibited a reduced methanol permeability compared to Nafion® [8]. All these examples constitutes the plausible support for P(AA-AMPS) as the promising candidate.

In summary, the objective of this study was to reduce the methanol crossover and increase the proton conductivity simultaneously by fabricating an ionic cross-linked interpenetrating network using a cationic polymer (chitosan) with a low alcohol permeability and an anionic polymer (P(AA-AMPS)) with a high proton conductivity.

2. Experimental

2.1. Materials and chemicals

Chitosan (CS) with a degree of deacetylation of 90% was supplied by Zhejiang Golden-shell biochemical Co., Ltd. P(AA-AMPS) with an average molecular weight of 5000 Da and a monomer mole ratio (AA:AMPS) of 9:1 was purchased from Shandong Taihe Water Treatment Co., Ltd. Formic acid, sulfuric acid and methanol was purchased locally. De-ionized water was used throughout the study.

2.2. Membrane preparation

CS was dissolved in 7 wt.% aqueous formic acid under stirring at 80 °C to get a 2 wt.% homogeneous CS solution. A desired amount of 2 wt.% P(AA-AMPS) aqueous solution was added dropwise to the above CS solution under constant stirring for 1 h. The mixture was then cast on a clean glass plate and dried at room temperature for about 48 h. The resulting membrane was immersed in 2 M H_2SO_4 solution for 24 h to allow cross-linking. The membrane was repeatedly rinsed with distilled water before being dried in a vacuum oven at 25 °C for 48 h. The membranes thus prepared were designated as CS/P(AA-AMPS)-*X* where *X* indicated the weight percentage of P(AA-AMPS) in the composite membrane (0–41 wt.%). The thickness of resulting membranes was in the range of 45–60 μm. When the content of P(AA-AMPS) exceeded 41 wt.%, precipitation occurred immediately upon mixing.

2.3. Characterizations

The membranes prepared were stored in a dry state prior to the Fourier transform infrared (FT-IR), X-ray photoelectron spectroscopy (XPS) and X-ray diffraction (XRD) analysis.

2.3.1. Fourier transform infrared (FT-IR)

The FT-IR spectra of CS and CS/P(AA-AMPS) membranes were recorded using a Nicolet-740, PerkinElmer-283B FT-IR Spectrometer.

2.3.2. X-ray photoelectron spectroscopy

The existing forms of the element nitrogen and the content of element sulfur were characterized by XPS using a PHI 1600 spectrometer with an Mg Kα radiation for excitation.

2.3.3. X-ray diffraction (XRD)

The crystalline structure of the membranes was investigated with a RigakuD/max2500v/pa X-ray diffractometer (Cu Kα 40 kV, 200 mA, 2° min^{-1}). The peak position and its area were extracted with MDIjade5 software. The chitosan crystallinity and the overall crystallinity were calculated by Eqs. (1) and (2)

[28].

$$\text{chitosan crystallinity (\%)} = \frac{\text{total area of CS crystalline peaks}}{\text{total area of CS peaks}} \times 100 \quad (1)$$

$$\text{overall crystallinity (\%)} = \frac{\text{total area of crystalline peaks}}{\text{total area of all peaks}} \times 100 \quad (2)$$

The areas of the CS crystalline peaks at 11.6°, 18.3°, 23.7° and 26.5° were taken into calculation of the total area of CS crystalline peaks. The crystalline peaks of the membrane at 11.6°, 18.3°, 21.4°, 23.7°, 26.5° and 27.9° were included in the calculation of the overall crystallinity.

2.3.4. Thermal analysis

The thermal analysis of the membranes was performed using a differential scanning calorimetry (DSC, PerkinElmer PYRIS Diamond) and thermal gravimetric analysis (TGA, PerkinElmer TG/DTA) under a nitrogen atmosphere at 10 °C min^{-1}. All the membrane samples were stored in a vacuum oven at 30 °C before analysis.

2.4. Water/methanol uptake and swelling degree

The water uptake and methanol uptake of the membranes were determined by measuring the membrane weight difference before and after immersion in water or in a methanol solution of 12 M for 24 h. The membrane was wiped with a filter paper to remove the water on the surface and weighted (W_{wet}). The same membrane sample was then dried in a vacuum oven at 60 °C for 24 h and weighted (W_{dry}). The water or methanol uptake was calculated using Eq. (3).

$$\text{uptake (wt.\%)} = \frac{W_{wet} - W_{dry}}{W_{dry}} \times 100 \quad (3)$$

where W_{wet} and W_{dry} are the weights of wet and dry membrane samples, respectively.

The swelling behavior of the membranes was studied by immersing the membrane sample of a size of 4 cm × 4 cm in water at room temperature for 24 h and measuring the area and volume change of the sample. The swelling degree was calculated by:

$$\text{swelling (\%)} = \frac{X_{wet} - X_{dry}}{X_{dry}} \times 100 \quad (4)$$

where X_{wet} and X_{dry} are the areas or volumes of the wet and dry samples, respectively.

The measurement errors of the water/methanol uptake and the swelling degree were both within ±4%.

2.5. Oxidation experiments

The oxidation resistance of the prepared membranes was evaluated by immersing the membranes in a 3 wt.% H_2O_2 aqueous solution with stirring at 25 °C or 60 °C for 4 days. The weight loss of the membranes was measured at certain time intervals.

2.6. Ion exchange capacity (IEC)

IEC of the membrane was determined by titration method. The membrane in H^+ form was immersed in 2 M NaCl solution for 24 h to replace the H^+ by Na^+ completely. The remaining solution was then titrated with a 0.01 M NaOH solution using phenolphthalein as an indicator. The IEC value was calculated by Eq. (5),

$$\text{IEC (mmol g}^{-1}) = \frac{0.01 \times 1000 \times V_{NaOH}}{W_d} \quad (5)$$

where V_{NaOH} (L) is the volume of NaOH solution consumed in the titration and W_d (g) is the weight of the dry membrane sample. The measurements were carried out with an accuracy of 0.001 mmol g^{-1}.

2.7. Proton conductivity

The proton conductivity of the membranes in the horizontal direction was measured in two-point-probe conductivity cells by the AC impedance spectroscopy method. The membrane impedance was measured with a frequency response analyzer (FRA, Autolab PGSTST20) over a frequency range of 1–10^6 Hz with oscillating voltage of 10 mV. The test temperature was controlled by the water vapor from room temperature to 80 °C. Before measurement, the membrane was equilibrated in de-ionized water for 24 h. The proton conductivity of the membrane was calculated by Eq. (6),

$$\sigma(\text{S cm}^{-1}) = \frac{L}{AR} \quad (6)$$

where L is the distance between the two probes; A is the cross-sectional area of testing sample; and R is the membrane resistance derived from the low intersection of the high frequency semicircle on a complex impedance plane with the $Re(Z)$ axis.

2.8. Methanol permeability

The methanol permeability was measured with a diffusion cell at room temperature as described in ref. [28]. An aqueous methanol solution of 5 M was used as the feed. The membrane was hydrated in de-ionized water for 48 h before being clamped tightly between the two compartments, one of which was initially filled with water and the other filled with methanol solution. The change of methanol concentration in the water compartment was determined using a gas chromatography (Agilent 6820) equipped with a TCD detector and a DB624 column. The methanol permeability (P, cm^2 s^{-1}) was determined by Eq. (7),

$$P(\text{cm}^2\,\text{s}^{-1}) = \frac{SV_B L}{AC_{A0}} \quad (7)$$

where S is the slope of curve of concentration vs. time; V_B is the volume of the receipt compartment; C_{A0} is the initial methanol concentration; L and A are the thickness and area of the membrane, respectively. The measurement error was within ±2%.

3. Results and discussion

3.1. Characterizations

All the membranes prepared were transparent and free standing, and exhibited sufficient flexibility for testing. No observable phase separation was found.

3.1.1. FT-IR studies

The chemical structure of P(AA-AMPS), CS membrane and CS/P(AA-AMPS) membranes was characterized by FT-IR (Fig. 1). The absorption peaks at 638 cm^{-1}, 1053 cm^{-1} and 1219 cm^{-1} appeared in the spectrum of P(AA-AMPS) as shown in Fig. 1(a) were assigned to the sulfonic acid groups [23]. The peak at 1626 cm^{-1} was attributed to the bending vibration of amide group, and the peak at 1733 cm^{-1} was owing to the stretching of carbonyl groups [29]. A comparison between the IR spectrum of pure CS membrane and that of CS/P(AA-AMPS) membranes revealed a chemical structure difference between them (Fig. 1(b)). The peaks of the amide I band at 1652 cm^{-1} and the amide II band at 1554 cm^{-1} existed in the CS membrane shifted toward lower wave numbers, to 1643 cm^{-1} and 1541 cm^{-1}, respectively, after the addition of P(AA-AMPS). This shift was attributed to the hydrogen bonds formed between the cationic polyelectrolyte CS and the anionic polyelectrolyte P(AA-AMPS). Furthermore, the intensity of the amide II band peak became stronger with the increase of the P(AA-AMPS) content, indicating a greater amount of $–NH_3^+$ species [19]. The presence of $–NH_3^+$ indicated that the ionic cross-linking interaction occurred between the CS and the P(AA-AMPS) polymer chains. In addition, the shift of the characteristic peak of carbonyl groups from 1733 cm^{-1} in the P(AA-AMPS) polymer to 1713 cm^{-1} in the CS/P(AA-AMPS) membrane proved the existence of intermolecular hydrogen bonds. The existence of the intermolecular hydrogen bonds and the positively charged $–NH_3^+$ species in the PEC membrane confirmed the construction of an acid–base blend IPN.

3.1.2. XPS studies

XPS analysis of N 1s for CS and CS/P(AA-AMPS)-29 membranes were presented in Fig. 2. The membrane samples for XPS study were not crosslinked with sulfuric acid. The high-resolution N 1s core-level XPS spectrum was resolved into two distinguishable species according to the different states of the nitrogen atoms in different microenvironments. Peak fitting of the N 1s core-level XPS spectra was conducted. The peak at a binding energy of 399.4 eV was assigned to the N in the amino

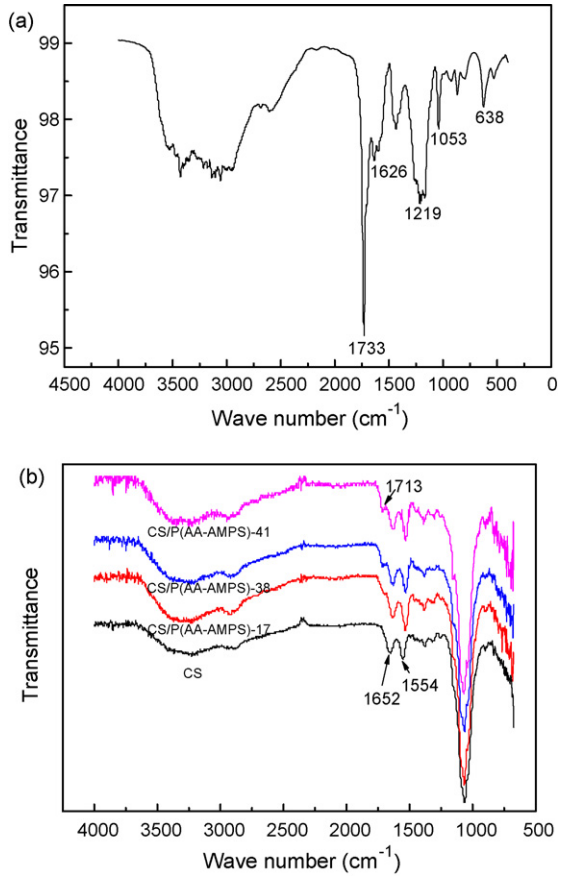

Fig. 1. FT-IR spectra of (a) P(AA-AMPS) polymer and (b) CS and CS/P(AA-AMPS) membranes.

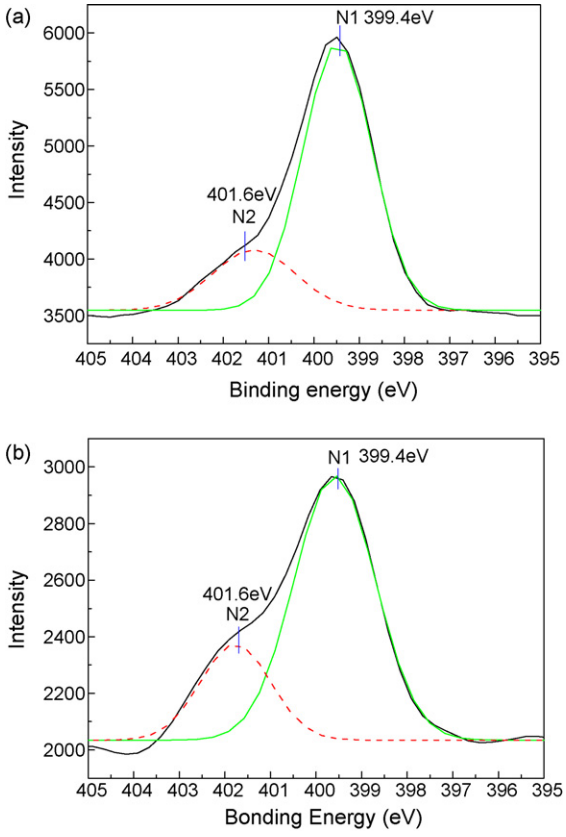

Fig. 2. High-resolution XPS spectra of N 1s for (a) CS and (b) CS/P(AA-AMPS)-29 membranes without cross-linking by H_2SO_4.

Table 1
N and S contents on the surface of CS and CS/P(AA-AMPS)-29 membranes

Membrane (uncrosslinked in H_2SO_4)	Experimental (%)		Theoretical (%)		Experimental (%)	Theoretical (%)
	N1	N2	N1	N2	S	S
CS	84.7	15.3	100.0	–	–	–
CS/P(AA-AMPS)-29	69.8	30.2	30.0	70.0	0.51	0.61

groups ($–NH_2$) of CS and the amido groups (–NH–C=O) of P(AA-AMPS). The other peak at a binding energy of 401.6 eV was assigned to the protonated amino groups ($–NH_3^+$) existed in the blend membranes. The experimental and theoretical amounts of N species and S species (not shown in the XPS spectra) were listed in Table 1. The content of N2 in the protonated amino form in the CS/P(AA-AMPS)-29 membrane was about 30.2% which was calculated by dividing the area of the peak at 401.6 eV by the total area of the N 1s peak. This content value was higher than that of pure CS membrane (15.3%), but lower than the theoretical value (70.0%) where a complete ionic interaction between the $–NH_2$ groups of CS and –COOH or $–SO_3H$ groups of P(AA-AMPS) was considered. It can be concluded from the above results that (i) an ionic cross-linked IPN did have been formed between the CS and the P(AA-AMPS),which was proved by the presence of the $–NH_3^+$ species; and (ii) not all but only part of the –COOH and $–SO_3H$ groups of P(AA-AMPS) took part in the ionic interaction. The excessive and free –COOH and $–SO_3H$ groups are supposed to form the proton transfer channels in the membrane.

The only slight difference between the measured S element content on the membrane surface and the theoretical value in terms of bulk content indicated that the two polyelectrolytes were blended homogeneously.

3.1.3. XRD studies

The XRD patterns of CS and P(AA-AMPS) membranes were shown in Fig. 3. Two forms of crystal structure of chitosan, form I (11.6°, 18.3°) and form II (21.3°, 23.7°), were found in this study, which was in agreement with ref. [30]. The broad peak at around 20° was attributed to the partly crystallized chitosan chains [28]. The characteristic crystal peaks of P(AA-AMPS) appeared at 11.6°, 17.6°, 21.4°, 23.6° and 28.1°. Comparing the XRD patterns of the pure CS membrane and the PEC membrane, it could be found that the intensity of the peaks at 21.4°, 23.6° and 27.9° increased with the increase of P(AA-AMPS) content, suggesting the effect of P(AA-AMPS) in interfering the arrangement of chitosan chains.

The calculated chitosan crystallinity and the overall crystallinity of CS/P(AA-AMPS) membranes were shown in Fig. 4. The chitosan crystallinity decreased with the increase of P(AA-AMPS) content, while the overall crystallinity of the membrane increased. The addition of P(AA-AMPS), on the one hand, destroyed the ordered packing of CS chains through the formation of hydrogen bonds and ionic interactions between the –COOH or $–SO_3H$ groups of P(AA-AMPS) and the –OH or $–NH_2$ groups of CS, leading to a decrease in chitosan crystallinity. On the other hand, the ionic cross-linking in the acid–base blend resulted in a more ordered arrangement of polymer chains, which was thought to be favored for rejecting the methanol permeation.

3.1.4. Thermal analysis

The TGA curves of the membranes and the P(AA-AMPS) polymer were shown in Fig. 5. TGA analysis showed a two-stage weight loss procedure of chitosan matrix membranes. The initial 10–15 wt.% weight loss took place between 30 °C and 150 °C, and the second weight loss started around 225 °C. The first weight loss stage was attributed to the loss of water contained in the membrane sample, and the membrane would be anhydrous above 150 °C. The second weight loss stage (225–350 °C) of the pure CS membrane was 48 wt.% due to the degradation of

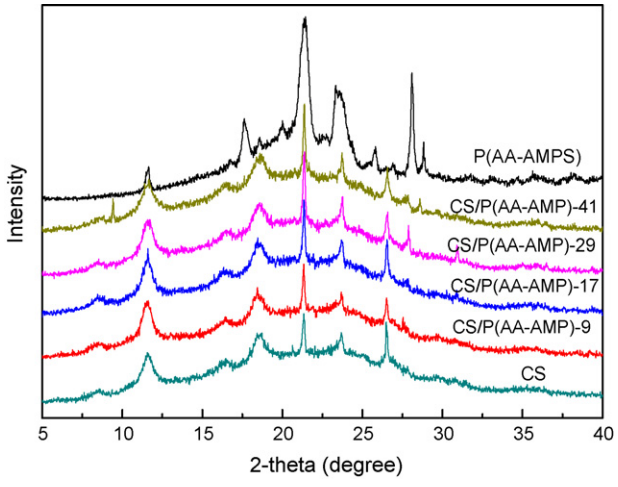

Fig. 3. XRD patterns of P(AA-AMPS) polymer, CS and CS/P(AA-AMPS) membranes.

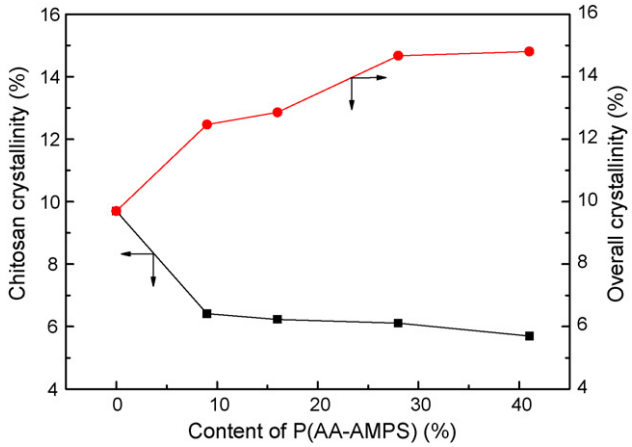

Fig. 4. Chitosan crystallinity and overall crystallinity of membranes.

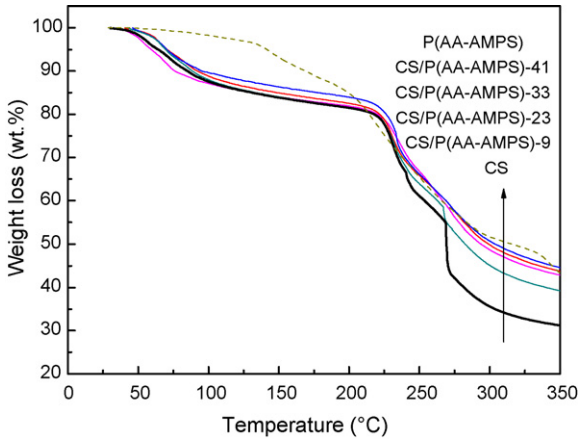

Fig. 5. TGA curves of P(AA-AMPS) polymer, CS and CS/P(AA-AMPS) membranes.

the chitosan chains [15]. The P(AA-AMPS) polymer exhibited a lower thermal stability with a degradation starting at 150 °C. For the CS/P(AA-AMPS) blend membranes, the degradation stage of P(AA-AMPS) at 150 °C was not observed and the second stage of decomposition was in the temperature range of 225–350 °C with a weight loss of 35–40 wt.% which was much lower than that of CS membrane. The enhanced thermal stability of the PEC membranes was attributed to the ionic cross-linked IPN structure. The CS/P(AA-AMPS) membranes were thermally stable up to 200 °C, that is, stable enough for application in DMFCs within the medium operating temperature range.

To further investigate the water retention ability of membranes with different P(AA-AMPS) content, DSC thermograms on the first run were recorded and analyzed (Fig. 6). As the content of P(AA-AMPS) increased, the endothermic peak due to the loss of water moved toward higher temperatures, from 78.6 °C to 91.0 °C when the content of P(AA-AMPS) increased from 0 wt.% to 41 wt.%. This elevated temperature revealed a stronger ability in water retention of the PEC membranes than CS, indicating a higher proton conductivity at higher temperature.

The glass transition temperatures (T_g) of the membranes were obtained from the DSC thermograms on the second run as shown

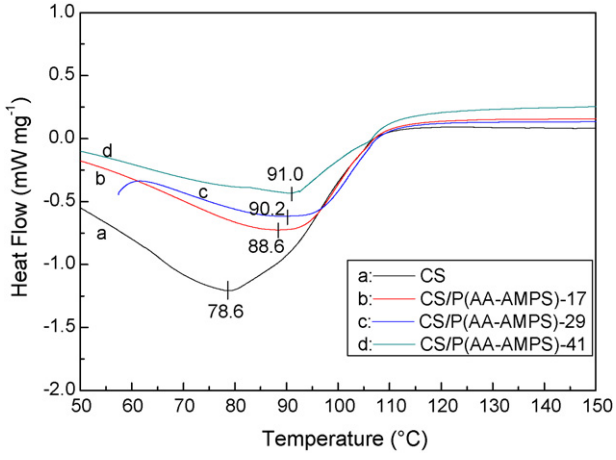

Fig. 6. DSC curves on the first run of CS and CS/P(AA-AMPS) membranes.

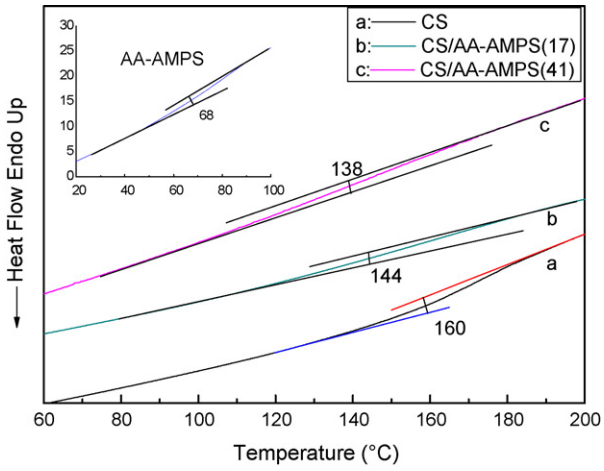

Fig. 7. DSC curves on the second run of CS and CS/P(AA-AMPS) membranes and P(AA-AMPS) polymer.

in Fig. 7. The T_gs of CS/P(AA-AMPS) membranes were found to be between that of CS (160 °C) and that of P(AA-AMPS) (68 °C). For polymer blends, the T_g is usually predicted by Fox equation without considering the interaction between the blend polymers [31]. The Fox equation assumes that the T_g depends only on the relative amounts of each polymer and on the T_g of the respective homopolymers, which is expressed by:

$$\frac{1}{T_g} = \frac{w_1}{T_{g1}} + \frac{w_2}{T_{g2}} \quad (8)$$

where w_1 and w_2 are the mass fractions of the two polymers; T_{g1}, T_{g2} and T_g are the glass transition temperatures of the two polymers and the blends, respectively.

The T_g values of CS/P(AA-AMPS)-17 and CS/P(AA-AMPS)-41 thus calculated were 141 °C and 106 °C, respectively, both lower than their corresponding experimental T_g values. The positive deviation between the measured and calculated values was due to the presence of the ionic cross-linked IPN. The permanent entanglement and chain interlocking in the IPN restricted the mobility of the polymer chains, resulting in an increased T_g. Furthermore, this positive deviation further increased from 3 °C to 32 °C when the content of P(AA-AMPS) increased from 17 wt.% to 41 wt.%. The larger the positive deviation was, the stronger the interaction in the membranes existed.

3.2. Water/methanol uptake and swelling degree

Water uptake, methanol uptake and swelling behavior of membranes play crucial roles in both the methanol permeability and the proton conductivity. The existence of water molecules in polyelectrolyte membranes significantly affects the transport of protons and the hydrated structures formed around the negatively charged fixed ions [32]. In this study, water uptake and methanol uptake of the membranes were measured and shown in Fig. 8(a). Both of the water uptake and the methanol uptake decreased with the increase of P(AA-AMPS) content as a result of the formed and enhanced ionic cross-linked IPN with the addition of P(AA-AMPS) which led to a decreased free volume in the membrane.

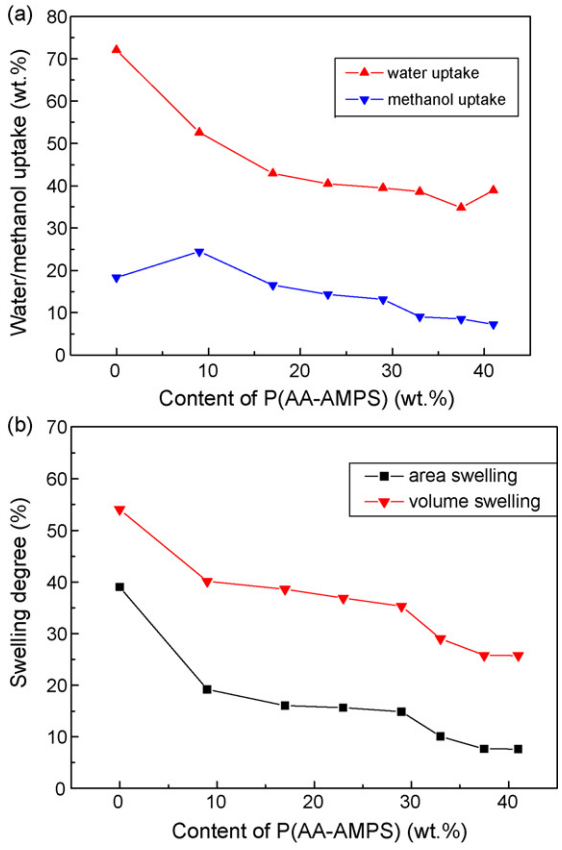

Fig. 8. Water/methanol uptake (a) and swelling degree (b) of CS and CS/P(AA-AMPS) membranes.

The water uptake of the blend membrane was much higher than the methanol uptake, indicating that the CS/P(AA-AMPS) membranes preferentially adsorbed water molecules over methanol molecules.

Swelling behavior of the membrane is an essential factor influencing the methanol permeation and the morphologic stability. Both the area and volume swelling were shown in Fig. 8(b). The swelling degree was notably lowered by the addition of anionic P(AA-AMPS). With the increase of P(AA-AMPS) content, the IPN structure of the PEC membrane formed, the mobility of the polymer chains as well as the free volume decreased, and the swelling was thereby inhibited.

3.3. Oxidative durability

The chemical and mechanical stability of the chitosan-based DMFC membranes has not been systematically investigated to our best of knowledge. Herein, the oxidative durability of pure chitosan membrane and CS/P(AA-AMPS) polyelectrolyte composite membrane were evaluated by exposing the membranes to a 3 wt.% H_2O_2 solutions at 25 °C or 60 °C, and the weight losses were shown in Table 2. The weight loss of CS membrane was found to be about 7 wt.% and 24 wt.% at 25 °C and 60 °C, respectively, after immersion for 24 h, whereas that of CS/P(AA-AMPS)-33 membrane was around 4 wt.% and 14 wt.% under the identical conditions, showing a higher oxidation resistance. The weight loss of pure CS membrane was 9 wt.% after immersion for 96 h at 25 °C, while at 60 °C, the CS membrane was broken into small pieces after immersion for 48 h. The weight loss of the CS/P(AA-AMPS)-33 membrane increased dramatically from 7 wt.% to 61 wt.% after 96 h immersion when the temperature was elevated from 25 °C to 60 °C. This increase was due to the much faster oxidation rate at higher temperatures. Comparing the stability of the pure CS membrane and the blend CS/P(AA-AMPS) polyelectrolyte composite membranes, it could be obviously concluded that the oxidative durability was improved by introducing the anionic P(AA-AMPS) into the cationic CS matrix to form an interpenetrating network.

Table 2
Weight loss of CS and CS/P(AA-AMPS)-33 membranes in 3 wt.% H_2O_2

Membrane	Weight loss (wt.%)							
	25 °C				60 °C			
	24 h	48 h	72 h	96 h	24 h	48 h	72 h	96 h
CS	7	8	9	9	24	Broken	–	–
CS/P(AA-AMPS)-33	4	7	7	7	14	29	42	61

3.4. Ion-exchange capacity

Ion-exchange capacity (IEC) indicates the amount of the ion exchangeable groups present in a polymer matrix which are responsible for proton transfer, and thus is an indirect and reliable approximation of the proton conductivity [19]. The calculated and experimental IEC values of CS, CS/P(AA-AMPS) polyelectrolyte complex membranes were listed and compared with Nafion®117 in Table 3. The IEC value of pure CS was 0.170 mmol g^{-1}, which was in agreement with that reported previously [15]. IEC^a_{cal}, IEC^b_{cal} and IEC_{exp} were, respectively, the IEC ignoring the ionic interaction, the IEC considering the ionic interaction and the measured values. Both the IEC^a_{cal} and the IEC^b_{cal} increased with the increasing content of P(AA-AMPS) while the IEC_{exp} increased gradually from 0.504 mmol g^{-1} to 0.894 mmol g^{-1}. The large difference between the IEC^a_{cal} and the IEC_{exp} was the result of the ionic cross-linked IPN that consumed part of the ion-exchange groups. The IEC_{exp}s were higher than or close to the IEC^b_{cal}s when the P(AA-AMPS) content was in the range of 9–41 wt.%. This was attributed to the uninteracted functional groups of –COOH and $–SO_3H$ as proved by the XPS studies. These unreacted –COOH and $–SO_3H$ groups in the membrane would contribute in increasing the proton conductivity. The IEC_{exp}s of the CS/P(AA-AMPS)-38 and CS/P(AA-AMPS)-41 membranes were close to that of Nafion®117 (0.852 mmol g^{-1}).

3.5. Proton conductivity

Proton conductivity is one of the most important properties for DMFCs membranes. The following two proton transfer mechanisms are commonly adopted in discussing the proton conductivity [33]: (I) Grotthus or "jump" mechanism which can be idealized as protons being passed down the chain of water molecules and ion exchange sites; and (II) vehicle mechanism

Table 3
IEC values of CS, CS/P(AA-AMPS) and Nafion® 117 membranes

Membrane	IEC_{cal}[a] (mmol g^{-1})	IEC_{cal}[b] (mmol g^{-1})	IEC_{exp} (mmol g^{-1})
Nafion® 117	0.909[c]	0.909	0.852
CS	–	–	0.170
CS/P(AA-AMPS)-9	1.09	0	0.504
CS/P(AA-AMPS)-17	2.00	0	0.551
CS/P(AA-AMPS)-23	2.77	0	0.589
CS/P(AA-AMPS)-29	3.43	0	0.726
CS/P(AA-AMPS)-33	4.00	0.27	0.833
CS/P(AA-AMPS)-38	4.50	1.01	0.841
CS/P(AA-AMPS)-41	4.94	1.65	0.894

[a] Ignoring the ionic interaction.
[b] Considering the ionic interaction.
[c] According to the equivalent weight of Nafion® 117 (1100 g mol^{-1} (–SO_3H)).

which assumes that protons combine with solvent molecules to yield complexes like H_3O^+ and then diffuse as a whole across the membrane. Generally, these two mechanisms exist simultaneously in the proton exchange membranes such as Nafion® 117 [33]. It has been found that the high conductivity of Nafion® membranes is due to the linked ionic cluster structure formed in the membrane [34], allowing the protons jump from one –SO_3H group to another through the channel in the presence of water. For CS/P(AA-AMPS) membranes, the proton transfer was supposed to be facilitated by the –COOH groups and –SO_3H groups. Meanwhile, the –NH_2 species also took part in the proton transfer. On the one hand, the –NH_2 species combined with water helped the formation of continuous hydrophilic regions [19,35,36] due to their inherent hydrophilic property. On the other hand, the basic –NH_2 group would interact with the –COOH or –SO_3H groups to form ionic bonds, consuming some of the proton exchange sites [5], which was not favorable for proton conductivity.

The proton conductivities of CS, CS/P(AA-AMPS) and Nafion® 117 membranes at 30 ± 3 °C were listed in Table 4. The proton conductivities of Nafion® 117 and CS reported in literatures were not always consistent due to the different test methods and conditions applied. In this study, Nafion® 117 and CS membranes showed proton conductivities of 6.96×10^{-2} S cm^{-1} and 2.02×10^{-2} S cm^{-1} near room temperature, respectively. The proton conductivity increased with the increase of the P(AA-AMPS) content from 9 wt.% to 41 wt.% and was in the range of 2.81×10^{-2} S cm^{-1} to 3.59×10^{-2} S cm^{-1}. This changing trend in proton conductivity was similar to the IEC results. Considering the water uptake property, it was interesting to notice that the membrane with a lower water uptake exhibited higher proton conductivity. Further studies on the proton conductivity at elevated temperatures were carried out.

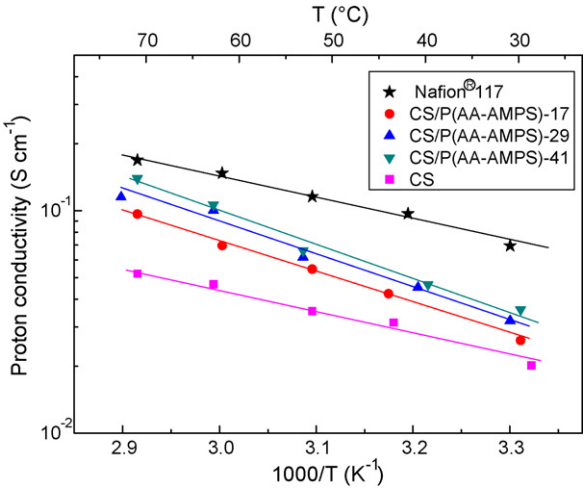

Fig. 9. Temperature dependence of proton conductivity of CS, CS/P(AA-AMPS) and Nafion® 117 membranes.

Fig. 9 showed the temperature dependence of proton conductivity of membranes under full hydration. The conductivity of the CS/P(AA-AMPS) membrane increased with increasing temperature from room temperature to 70 °C, owing to the good water retainability. Meanwhile, the samples were well hydrated during the test, and eliminated the effect of humidification [37]. The proton conductivity agreed with the Arrhenius law [9], indicating that the proton conduction was dominated by a thermal activation process. The activation energy (E_a) of conductivity for each membrane was estimated from the gradient of the fitting

Table 4
Proton conductivity of CS, CS/P(AA-AMPS) and Nafion® 117 membranes

Membrane	Conductivity (×10^{-2} S cm^{-1}, 30 ± 3 °C) Content of P(AA-AMPS) (wt.%)							
	0	9	17	23	29	33	38	41
Nafion® 117	6.96							
CS	2.02							
CS/P(AA-AMPS)		2.81	2.61	3.00	3.21	3.30	3.47	3.59

Table 5
Activation energy of conductivity of CS, CS/P(AA-AMPS) and Nafion®117 membranes

Membrane	Thickness (μm)	E_a (kJ mol^{-1})
CS	64	7.9
CS/P(AA-AMPS) −17	65	11.7
CS/P(AA-AMPS) −29	60	12.6
CS/P(AA-AMPS) −41	64	13.3
Nafion®117	190	9.2

line by the following equation and presented in Table 5.

$$\sigma = \sigma_o \exp\left(-\frac{E_a}{RT}\right) \quad (9)$$

The E_a values for CS/P(AA-AMPS) membranes were found to be between 11.7 kJ mol^{-1} and 13.3 kJ mol^{-1}, higher than that for Nafion®117 (9.2 kJ mol^{-1}) but lower than that for only "jump" mechanism which was reported to be around 14–40 kJ mol^{-1} [9]. It was deduced that both the "Grotthus" mechanism and vehicle mechanism existed in the PEC membranes as illustrated in Scheme 1. The low activation energy of conductivity implied that continuous hydrophilic channels (the shadowed region in Scheme 1) were most probably constructed in the PEC membrane to facilitate proton transfer, especially in the complex membrane with a lower P(AA-AMPS) content. The hydrophilic CS and P(AA-AMPS) both contributed to the formation of these water channels. A part of protons combined with water molecules generating such clusters as H_3O^+, and transferred through the water channels in the membranes (as shown in Scheme 1(a)). The other part of protons transferred along the ionic bonds and hydrogen bonds by "jumping" from one function group to another as shown in Scheme 1(b). The addition of P(AA-AMPS) brought in extra ion exchange groups including the weak acidic –COOH groups and the strong acidic $–SO_3H$ groups. The resultant hydrogen bonds and ionic bonds between the acid groups on P(AA-AMPS) and the –OH or $–NH_2$ groups on CS enhanced the proton transport controlled by the "Grotthus" mechanism. In other words, a proton-conducting pathway was constructed and the distance between the hopping sites was shortened by the IPN structure with a high density of –COOH and $–SO_3H$ groups in the complex membrane. Moreover, the E_a for proton conductivity increased with increasing the P(AA-AMPS) content. The decreased water uptake and amorphous regions in the membrane led to a decrease in water flux. Therefore, the Grotthus mechanism became more predominant at higher P(AA-AMPS) contents.

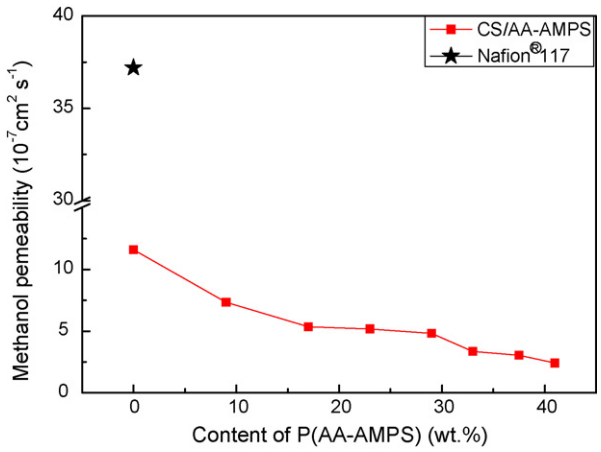

Fig. 10. Methanol permeability of CS, CS/P(AA-AMPS) and Nafion®117 membranes.

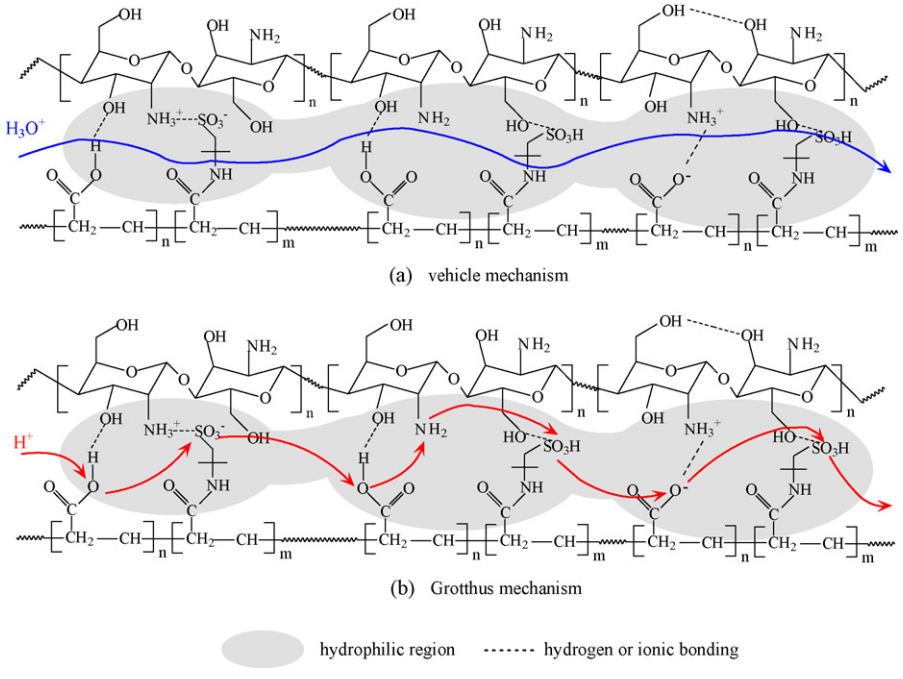

Scheme 1. Tentative illustration of the proton transfer mechanism in CS/P(AA-AMPS) membranes: (a) vehicle mechanism (b) Grotthus mechanism.

3.6. Methanol permeability

Methanol permeability is another essential property for DMFC-oriented membranes. The methanol permeability of the membranes prepared and Nafion® 117 was shown in Fig. 10. The methanol crossover was greatly dependent on the structure of the membrane [38] and the specific interaction between water and membrane [39]. It has been found that the partition coefficient of methanol between Nafion® membrane and the solution was constant below 90 °C, which was regardless of the methanol feed [40]. The higher methanol permeability for Nafion®117 was associated with swelling property. Although the water uptake of Nafion®117 (19 wt.%) was lower than that of chitosan matrix membrane, the amount of loosely bound or free water might be higher than the CS membrane [39]. The methanol permeability of Nafion®117 was measured to be 37.2×10^{-7} cm^2 s^{-1} for 5 M methanol feed, three times higher than pure CS membrane (11.60×10^{-7} cm^2 s^{-1}) under the same testing conditions.

Besides the fact that chitosan is a good methanol barrier material which has been proved in alcohol/water separations, the dense ionic crosslinked IPN formed in the blends of chitosan and P(AA-AMPS) is supposed to further reduce the methanol crossover. Most of sulfonated membranes exhibited enhanced proton conductivity but higher methanol crossover with the increase of sulfonation degree, showing a so-called trade-off effect [38]. However, the PEC membranes prepared in this study showed an reversal trade-off effect, that is, the methanol permeability decreased with the increase of P(AA-AMPS) content as anticipated. The decreased amorphous regions led to a decrease in the methanol and water flux, and the IPN preferentially adsorbed water over methanol. As a result, the methanol crossover was diminished. Meanwhile, the compact structure resulted from the strong ionic interactions between the $–NH_2$ groups of CS and the –COOH or $–SO_3H$ groups of P(AA-AMPS) also led to a decrease in methanol permeability. Additionally, the methanol permeability of CS/P(AA-AMPS) membranes changed only slightly when the P(AA-AMPS) content was higher than 30 wt.%. This may be ascribed to the fact that a stable IPN structure was constructed which was composed by a large number of ionic bonds and hydrogen bonds between P(AA-AMPS) and chitosan, and further increase in P(AA-AMPS) content exerted little influence on this structure.

3.7. Selectivity ($\beta = \sigma/P$)

The efficiency for separating two components by some membrane separation processes, such as by pervaporation and gas separation, is usually evaluated by selectivity, an index defined as the ratio of the permeation flux of the two components [41]. For the membranes in DMFC application, a similar index can be defined if the membrane is viewed as a proton/methanol separation medium. When the Nernst–Plank equation and the Fick's law are applied in describing the proton flux and the methanol flux, respectively, the H^+/methanol selectivity (β) can be expressed in the form of $\beta = \sigma/P$, i.e., the ratio of proton conductivity (σ) to methanol permeability (P). Although this index alone is not sufficient to evaluate the membrane performance, it is often used to describe and compare the total performances of various membranes.

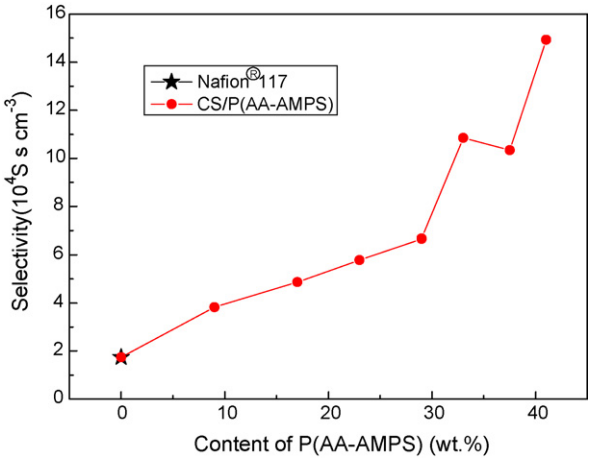

Fig. 11. Selectivity of CS, CS/P(AA-AMPS) and Nafion®117 membranes.

Fig. 11 showed the selectivities of the CS/P(AA-AMPS) membranes and Nafion®117, which were determined based on their conductivities and methanol permeabilities measured at 30 °C. It can be found that all the blend membranes fabricated in this study had a higher selectivity than Nafion®117. The selectivity increased with the content of P(AA-AMPS), and at P(AA-AMPS) content of 41 wt.% the highest value of 15.0×10^4 S s cm^{-3} was obtained. The increased selectivity should be ascribed to the dual function of the incorporated P(AA-AMPS) polymer, which increased the proton conductivity and decreased the methanol crossover. The high selectivity of the blend CS/P(AA-AMPS) membranes, up to about eight times higher than Nation 117, implied a promising application potential for DMFCs.

4. Conclusions

A novel PEC membrane was developed by blending the cationic polyelectrolyte, chitosan, with the anionic polyelectrolyte, P(AA-AMPS). Chitosan was chosen as a good methanol barrier material and P(AA-AMPS) as a proton-conducting component. An ionic cross-linked IPN structure was established between the two polymers. The desirable results were achieved that the methanol permeability was reduced while the proton conductivity was increased with the increase of the of P(AA-AMPS) content. The highest proton conductivity of 3.59×10^{-2} S cm^{-1} and the lowest methanol permeability of 2.41×10^{-7} cm^2 s^{-1} were observed when the P(AA-AMPS) content was 41 wt.%. Accordingly, a high selectivity ($\beta = \sigma/P$) was obtained, which was eight times higher than that for Nafion®117. The mechanism of proton transfer was tentatively discussed based on the activation energy of conductivity. Both of the two mechanisms, Grotthus or "jump" mechanism and vehicle mechanism, occurred in the membrane and the former seemed to be of predominance. This kind of PEC membranes

jointly employing the methanol-rejecting property of one polyelectrolyte and the proton-conducting property of the other polyelectrolyte shows a promising application potential for DMFCs.

Acknowledgements

We gratefully acknowledge financial support from the National Nature Science Foundation of China (No. 20776101), the Programme of Introducing Talents of Discipline to Universities (No. B06006) and the Cross-Century Talent Raising Program of Ministry of Education of China, the Program for Changjiang Scholars and Innovative Research Team in University (PCSIRT). We thank Professor Yuxin Wang for his help in the proton conductivity measurements.

References

[1] V. Neburchilov, J. Martin, H. Wang, J. Zhang, J. Power Sources 169 (2007) 221–238.
[2] A. Heinzel, V.M. Barragán, J. Power Sources 84 (1999) 70–74.
[3] Y. Yang, Z. Shi, S. Holdcroft, Macromolecules 37 (2004) 1678–1681.
[4] B. Smitha, S. Sridhar, A.A. Khan, Eur. Polym. J. 41 (2005) 1859–1866.
[5] C. Zhao, Z. Wang, D. Bi, H. Lin, Polymer 48 (2007) 3090–3097.
[6] S. Zhonga, X. Cui, H. Cai, H. Na, J. Power Sources 168 (2007) 154–161.
[7] F. Schönberger, M. Hein, J. Kerres, Solid State Ionics 178 (2007) 547–554.
[8] C.W. Walker, J. Electrochem. Soc. 151 (2004) A1797–A1803.
[9] C.W. Lin, Y.F. Huanga, A.M. Kannanb, J. Power Sources 171 (2007) 340–347.
[10] M. Matsuguchi, H. Takahashi, J. Membr. Sci. 281 (2006) 707–715.
[11] K.Y. Cho, H.Y. Jung, S.S. Shin, N.S. Choi, Electrochim. Acta 50 (2004) 589–593.
[12] Y. Zhai, H. Zhang, Y. Zhang, D. Xing, J. Power Sources 169 (2007) 259–264.
[13] C.W. Lin, R. Thangamuthu, C.J. Yang, J. Membr. Sci. 253 (2005) 23–31.
[14] P. Mukoma, B.R. Joosteb, H.C.M. Vosloo, J. Membr. Sci. 243 (2004) 293–299.
[15] P. Mukoma, B.R. Jooste, H.C.M. Vosloo, J. Power Sources 136 (2004) 16–23.
[16] S.K. Choudhari, A.A. Kittur, S.S. Kulkarni, M.Y. Kariduraganavar, J. Membr. Sci. 302 (2007) 197–206.
[17] X. Wu, G. He, S. Gu, Z. Hu, P. Yao, J. Membr. Sci. 295 (2007) 80–87.
[18] S. Jin, M. Liu, F. Zhang, S. Chen, Polymer 47 (2006) 1526–1532.
[19] B. Smitha, S. Sridhar, A.A. Khan, Macromolecules 37 (2004) 2233–2239.
[20] C.S. Harris, T.G. Rukavina, Electrochim. Acta 40 (1995) 2315–2320.
[21] Y.H. Huang, L.C. Chen, K.C. Ho, Solid State Ionics 165 (2003) 269–277.
[22] J.P. Randin, J. Electrochem. Soc. 129 (1982) 1215–1220.
[23] J. Qiao, T. Hamaya, T. Okada, Polymer 46 (2005) 10809–10816.
[24] T. Hamaya, S. Inoue, J. Qiao, T. Okada, J. Power Sources 156 (2006) 311–314.
[25] J. Qiao, S. Ikesaka, M. Saito, J. Kuwano, T. Okada, Electrochem. Commun. 9 (2007) 1945–1950.
[26] Y. Shen, J. Xi, X. Qiu, W. Zhu, Electrochim. Acta 52 (2007) 6956–6961.
[27] C.W. Walker, J. Power Sources 110 (2002) 144–151.
[28] W. Yuan, H. Wu, B. Zheng, X. Zheng, Z. Jiang, J. Power Sources 172 (2007) 604–612.
[29] C. Hu, B. Li, R. Guo, H. Wu, Z. Jiang, Sep. Purif. Tech. 55 (2007) 327–334.
[30] X. Chen, H. Yang, Z. Gu, Z. Shao, J. Appl. Polym. Sci. 79 (2001) 1144–1149.
[31] R. Paris, J.L. de la Fuente, J. Polym. Sci.: Part B: Polym. Phys. 45 (2007) 1845–1855.
[32] T.L. Kalapos, B. Decker, H.A. Every, H. Ghassemi, T.A. Zawodzinski Jr., J. Power Sources 172 (2007) 14–19.
[33] B.S. Pivovar, Y. Wang, E.L. Cussler, J. Membr. Sci. 154 (1999) 155–162.
[34] J.Y. Li, S.N. Nasser, Mech. Mater. 32 (2000) 303–314.
[35] Y. Wan, K.A.M. Creber, B. Peppley, V.T. Bui, Polymer 44 (2003) 1057–1065.
[36] J.R. Salgado, Electrochim. Acta 52 (2007) 3766–3778.
[37] X. Ren, M.S. Wilson, S. Gottesfeld, J. Electrochem. Soc. 143 (1996) L12–L15.
[38] R. Jiang, H.R. Kunz, J.M. Fenton, J. Electrochem. Soc. 153 (2006) A1554–A1561.
[39] Y.S. Kim, M.J. Sumner, W.L. Harrison, J.S. Riffle, J.E. McGrath, B.S. Pivovar, J. Electrochem. Soc. 151 (2004) A2150–A2156.
[40] X. Ren, T.E. Springer, T.A. Zawodzinski, S. Gottesfeld, J. Electrochem. Soc. 147 (2000) 466–474.
[41] B. Libby, W.H. Smyrl, E.L. Cussler, AIChE J. 49 (2003) 991–1001.